Robust Control Applications for Smart Truss Structure

Ricardo Carvalhal, Samuel da Silva and Vicente Lopes Júnior
Universidade Estadual Paulista
Department of Mechanical Engineering – UNESP – Ilha Solteira
Av. Brasil Centro, 56, Ilha Solteira, São Paulo, 15385-000, Brazil
e-mail: ricardoc@dem.feis.unesp.br

ABSTRACT

A finite element modeling of an intelligent truss structure with piezoelectric stack actuators for the purpose of active damping and structural vibration attenuation is presented. This paper concerns with the following issues aspects: the design of intelligent truss structure considering electro-mechanical coupling between the host structure and piezoelectric stack actuators; the H_2 norm approach to search for optimal placement of actuators and sensors; and finally some aspects in robust control techniques. The electro-mechanical behavior of piezoelectric elements is directly related to the successful application of the actuators in truss structures. In order to achieve the desired damping in the interested bandwidth frequency it is used the H_∞ output feedback solved by convex optimization. The constraints to be reached are written by linear matrix inequalities (LMI). The paper concludes with a numerical example, using Matlab and Simulink, in a cantilevered, 2-bay space truss structure. The results demonstrated the approach applicability.

NOMENCLATURE

$\mathbf{k}^e$	local mechanical-electric stiffness matrix for the piezoelectric active member
k_2, c_2, $\bar{c}_2$	see eq.(2)
E	elastic modulus
A	cross-section area
L	length
e	piezoelectric coefficient
ε	dielectric coefficient
$\boldsymbol{q}$, $\dot{\boldsymbol{q}}$, $\ddot{\boldsymbol{q}}$	physical responses
$\mathbf{M}$, $\mathbf{D}$, $\mathbf{K}$	mass, damping, stiffness matrix
$\boldsymbol{Q}$	control coefficient matrix
$\boldsymbol{V}$	applied voltage vector
$\boldsymbol{F}$	load force vector
$\mathbf{A}$, $\mathbf{B}_1$, $\mathbf{B}_2$, $\mathbf{C}$	see eq.(4)
$\boldsymbol{w}$	disturbance input
$\boldsymbol{u}$	control input
$\boldsymbol{y}$	output
$\boldsymbol{x}$, $\boldsymbol{xi}$	state vector, ith state component
$\boldsymbol{q_i}$, $\dot{\boldsymbol{q}}_i$	modal displacement, velocity
$\boldsymbol{q_{mi}}$	see eq.(5)
ζ_i, ω_i	modal damping, natural frequency
n	number of modelled modes
$\mathbf{A_{mi}}$, $\mathbf{B}_{mi}$, $\mathbf{C_{mi}}$	see eq.(6)
$\|\cdot\|_2$, $\|\cdot\|_\infty$	2-norm, infinity-norm
Tr(.)	matrix trace
$\mathbf{R}$	see eq.(8)
σ_{ik}	placement index
s	number of actuator
m	number of considered modes
$\mathbf{T}$	placement matrix
$\boldsymbol{z}$	regulated output
$\mathbf{K}$	output feedback controller
$\boldsymbol{p}$	output of the feedback perturbation
$\boldsymbol{r}$	input vector
Δ	unknown but bounded
$\mathbf{P}$	generalized plant
λ	design cost
$\mathbf{P_{ij}}$	see eq.(11)
$\mathbf{G}$, $\mathbf{G_p}$, $\mathbf{G_r}$, $\mathbf{G_c}$	transfer function
$\boldsymbol{K_d}$	attenuation constant
$\mathbf{W_y}$, $\mathbf{W_u}$	filters
$\mathbf{H_{ij}}$	see eq.(17)
$\mathbf{K_w}$	attenuation gain
$\mathbf{S}$	sensitivity function
$\mathbf{U}$	Energy restriction function

INTRODUCTION

Lightweight space structures are the future of space vehicles and satellite technology. Possessing ideal space launching characteristics, such as minimal storage volume and minimal mass, these lightweight structures will propel the space industry into the next generation of space satellite technology. Space satellites must be expertly controlled from a vibration standpoint because signal transmission to and from the earth mandates tight tolerances. Vibration control is critical to mission success as well as satellite longevity [1].

Large and light space structures are basically flexible due to their low stiffness and damping. This creates a problem since flexible structures present many vibratory modes within or beyond the bandwidth of the controller. When only a few modes are dealt with in the control, spillover may occur because uncontrolled higher modes or unmodelled modes may become excited. The effects of spillover are worse where the structure, sensors or actuators are poorly modelled and the numbers of sensors and actuators are low.

In order to achieve better dynamic properties of the structure, great attention has been paid to the control of structural vibration using smart structures. So, the application of active vibration control in flexible structures has been increasingly used as a solution for space structures, in order to achieve the degree of vibration attenuation required for precision pointing accuracy and to guarantee the stability.

The active members are integrated into the structure at a high degree because of their multiple functions: they serve as structural elements with load carrying capacities; as actuators, which exert internal forces; and as sensor elements allowing measurement of the elastic strains. The piezoelectric stack actuators are remarkable because they are light weight, high force and low power consumption [2].

Several researchers have proved that piezoelectric material can be effective in active vibration control. In truss structures the control force can be accomplished by piezoelectric active members, known as “PZT wafer stacks”, that are mechanically linked in series producing an axial force in the bar that are positioned.

An important stage in the design of structures is the sensor/actuator placement. The location of the sensors affects the trustiness of the signal generated by it and the location of the actuators minimizing the control efforts. Practically, actuators used in intelligent structures are more massive than sensors. Therefore, optimal placement of actuators, which implicitly minimizes the number of required actuators, has a great significance especially for space applications [3]. In this work, the optimal placement of active members considers the determination of the H_2 norm for each sensor/actuator candidate position for selected modes of the system.

The design of H_∞ output feedback control laws that meet desired performance and/or robustness specifications is an active research area of the control community for several decades. The cost functions used in H_∞ control are very general and can directly include performance specifications, disturbance rejection specifications, control input magnitude limitations and robustness requirements. The strength of these design methodology is the generality of the cost function [4]. In this work, the problem of H_∞ output feedback control is solved by convex optimization and is written through linear matrix inequalities (LMI).

EQUATIONS OF MOTION FOR PIEZELETRIC SMART TRUSS

A smart truss structure is composed of active and passive members. The formulation of passive members is easily obtained by finite elements and it is very useful in the formulation of active members, which are commonly composed of a piezoelectric stack and two metallic bars. The stiffness matrix for an active member is formulated by assembling the stiffness matrix for the piezoelectric stack with the well-known stiffness matrices of the two metallic bars, considering that each piezoelectric active member has one electric degree of freedom. The local mechanical-electric stiffness matrix for the piezoelectric active member, described in [5], is:

$$\mathbf{k^e} = \begin{bmatrix} \dfrac{k_1k_2k_3}{k_1k_2+k_1k_3+k_2k_3} & \dfrac{-k_1k_2k_3}{k_1k_2+k_1k_3+k_2k_3} & \dfrac{-k_1c_2k_3}{k_1k_2+k_1k_3+k_2k_3} \\ \dfrac{-k_1k_2k_3}{k_1k_2+k_1k_3+k_2k_3} & \dfrac{k_1k_2k_3}{k_1k_2+k_1k_3+k_2k_3} & \dfrac{k_1c_2k_3}{k_1k_2+k_1k_3+k_2k_3} \\ \dfrac{-k_1c_2k_3}{k_1k_2+k_1k_3+k_2k_3} & \dfrac{k_1c_2k_3}{k_1k_2+k_1k_3+k_2k_3} & \dfrac{-c_2^2(k_1+k_3)}{k_1k_2+k_1k_3+k_2k_3} - \bar{c}_2 \end{bmatrix} \tag{1}$$

$$k_2 = E_2A_2 \big/ L_2, \quad c_2 = e_2A_2 \big/ L_2, \quad \bar{c}_2 = \varepsilon_2A_2 \big/ L_2 \tag{2}$$

where e is the piezoelectric coefficient, ε is the dielectric coefficient, E is the elastic modulus, A is the cross-section area and L is the length of each part of the elements. The subscripts *1*, *2* and *3* correspond to the left metallic bar, piezoelectric stack and right metallic bar, respectively; and k_1 and k_3 are defined analogously to k_2 in eq. (2).

Assembling the equations of motion of the truss structure with piezoelectric members and common metal members in global coordinate, the global equations of motion for a smart truss structure is given by:

$$\mathbf{M}\ddot{\boldsymbol{q}} + \mathbf{D}\dot{\boldsymbol{q}} + \mathbf{K}\boldsymbol{q} = \boldsymbol{F} - \mathbf{Q}\boldsymbol{V} \tag{3}$$

where $\boldsymbol{q}$, $\dot{\boldsymbol{q}}$ and $\ddot{\boldsymbol{q}}$ are the displacement, velocity and acceleration vectors, respectively; **M**, **D** and **K** are the mass, the damping, and the stiffness matrices, respectively; **Q** is the control coefficient matrix that is related to the actuator control force applied to the corresponding nodal degree of freedom; $\boldsymbol{V}$ is the applied voltage vector of the smart structure and $\boldsymbol{F}$ is the load force vector.

For control system analysis and design purposes, it is convenient to represent the flexible structure equations in a state-space form:

$$\dot{\boldsymbol{x}} = \mathbf{A}\boldsymbol{x} + \mathbf{B}_1\boldsymbol{w} + \mathbf{B}_2\boldsymbol{u}, \quad \boldsymbol{y} = \mathbf{C}\boldsymbol{x} \tag{4}$$

where **A** is the dynamic matrix, $\mathbf{B}_1$ is the matrix of disturbance input, $\mathbf{B}_2$ is the matrix of control input, **C** is the output matrix, $\boldsymbol{w}$ is the vector of disturbance input, $\boldsymbol{u}$ is the vector of control input, and $\boldsymbol{y}$ is the output vector.

The state vector $\boldsymbol{x}$ of the modal coordinates consist of n independent components, $\boldsymbol{xi}$, that represent a state of each mode. The $\boldsymbol{xi}$ (*ith* state component) can be given by:

$$\boldsymbol{xi} = \begin{Bmatrix} \boldsymbol{q_i} \\ \boldsymbol{q_{mi}} \end{Bmatrix}, \quad \text{where } \boldsymbol{q_{mi}} = \zeta_i\mathbf{q}_i + \dot{\mathbf{q}}_i \big/ \omega_i \tag{5}$$

where $\boldsymbol{q}_i$ is the *ith* modal displacement, $\dot{\boldsymbol{q}}_i$ is the *ith* modal velocity, ζ_i is the *ith* modal damping, ω_i is the *ith* natural frequency and n is the number of modeled modes.

The modal state-space realization is characterized by the block-diagonal dynamic matrix and the related input and output matrices:

$$\mathbf{A} = \text{blockdiag}(\mathbf{A_{mi}}), \quad \mathbf{B} = \begin{bmatrix} \vdots \\ \mathbf{B_{mi}} \\ \vdots \end{bmatrix}, \quad \mathbf{C} = \begin{bmatrix} \cdots & \mathbf{C_{mi}} & \cdots \end{bmatrix}, \quad \text{where } \mathbf{A_{mi}} = \begin{bmatrix} -\zeta_i\omega_i & \omega_i \\ -\omega_i & -\zeta_i\omega_i \end{bmatrix} \tag{6}$$

where the subscript $(.)_{mi}$ is relative to *ith* dynamic mode and $\mathbf{A}_{mi}$ is one possible form to block-diagonal dynamic matrix. More information about this topic can be found in [6].

The order of the state-space representation is generally very large, causing numeric difficulties. Therefore, the obtaining of a low order model is fundamental for a controller success. A reduced-order model can be obtained by truncating the states. Let $\boldsymbol{x}$ and the state ($\mathbf{A}$, $\mathbf{B}_1$, $\mathbf{B}_2$, $\mathbf{C}$) be partitioned considering the canonical modal decomposition. From the Jordan canonical form, it can be obtained:

$$\begin{Bmatrix} \dot{\boldsymbol{x}}_c \\ \dot{\boldsymbol{x}}_r \end{Bmatrix} = \begin{bmatrix} \mathbf{A}_c & \mathbf{0} \\ \mathbf{0} & \mathbf{A}_r \end{bmatrix} \begin{Bmatrix} \boldsymbol{x}_c \\ \boldsymbol{x}_r \end{Bmatrix} + \begin{bmatrix} \mathbf{B}_{1c} \\ \mathbf{B}_{1r} \end{bmatrix} \boldsymbol{w} + \begin{bmatrix} \mathbf{B}_{2c} \\ \mathbf{B}_{2r} \end{bmatrix} \boldsymbol{u}$$
$$\boldsymbol{y} = \begin{bmatrix} \mathbf{C}_c & \mathbf{C}_r \end{bmatrix} \begin{Bmatrix} \boldsymbol{x}_c \\ \boldsymbol{x}_r \end{Bmatrix} \tag{7}$$

where the subscripts $(.)_{\boldsymbol{c}}$ and $(.)_{\boldsymbol{r}}$ mean controlled modes and residual modes, respectively.

OPTIMAL PLACEMENT OF ACTIVE MEMBERS USING H_2 NORM

The norm of a system ($\mathbf{A}$, $\mathbf{B}$, $\mathbf{C}$) can be calculated by different forms. In this work the H_2 norm is calculated using linear matrix inequalities (LMI) and it is used as performance index. Assunção et al. [7] demonstrate in full detail as to compute this norm. The H_2 norm system can be found from the following optimization problem:

$$\|G\|_2^2 = min\ Tr\left(\mathbf{CRC}^{\mathbf{T}}\right)$$
$$\text{subject to : } \mathbf{AR} + \mathbf{RA}^{\mathbf{T}} + \mathbf{BB}^{\mathbf{T}} < 0 \quad \text{and} \quad \mathbf{R} > 0 \tag{8}$$

where $\mathbf{R}$ is a symmetric positive defined matrix, and Tr(.) is the trace of the matrix. The H_2 norm of a mode also corresponds to the area under the transfer function of this mode. The system H_2 norm value is approximately the sum of areas of each of the modes.

The optimal placement problem consists of determining the location of a small set of actuators and sensors such that H_2 norm system is the closest possible of the norm system using a large set of actuator and sensor, [6]. The H_2 placement index σ_{ik} evaluates the *kth* actuator (sensor) at the *ith* mode. It is defined in relation to every modes and every admissible actuators, as:

$$\sigma_{ik} = \frac{\|G_{ik}\|_2}{\|G\|_2}, \qquad k = 1,\cdots,s \qquad i = 1,\cdots,m \tag{9}$$

where s is the number of actuators and m is the number of considered modes. It is convenient to represent the placement index as a placement matrix:

$$\mathbf{T} = \begin{bmatrix} \sigma_{11} & \sigma_{12} & \cdots & \sigma_{1k} & \cdots & \sigma_{1S} \\ \sigma_{21} & \sigma_{22} & \cdots & \sigma_{2k} & \cdots & \sigma_{2S} \\ \cdots & \cdots & \cdots & \cdots & \cdots & \cdots \\ \sigma_{i1} & \sigma_{i2} & \cdots & \sigma_{ik} & \cdots & \sigma_{iS} \\ \cdots & \cdots & \cdots & \cdots & \cdots & \cdots \\ \sigma_{m1} & \sigma_{m2} & \cdots & \sigma_{mk} & \cdots & \sigma_{mS} \end{bmatrix} \Leftarrow \textit{ith mode}$$
$$\Uparrow$$
$$\textit{kth actuator} \tag{10}$$

where the *kth* column consists of indexes of the *kth* actuator for each mode, and the *ith* row is a set of the indexes of the *ith* mode for each actuator. The H_2 norm has an additive property that the H_2 norm of a structure with a set of actuators is the rms sum of the H_2 norms of a structure with each single actuator from this set. The actuators with small indexes can be removed as the least significant ones. The largest value indexes are optimal position to consider an actuator. Similarly, it is possible to determine the optimal placement of the sensors.

H_∞ OUTPUT FEEDBACK CONTROL

A standard form of a general feedback system with uncertainty is given by Fig. 1, where ***w*** is the exogenous vector, ***z*** is the regulated output vector, ***y*** is the output signal used to feedback the system, **K** is the output feedback controller, ***u*** is the signal of control, ***p*** is the output of the feedback perturbation, Δ, and ***r*** is the input vector of the uncertainty block Δ. The uncertainty block Δ represents an unstructured perturbation and it is considered an unknown variable, but with bounded norm by $\|\Delta\|_\infty \leq 1$. The generalized plant **P** includes the dynamic information of the transfer function of the system and the respective interconnection between the input and output signals.

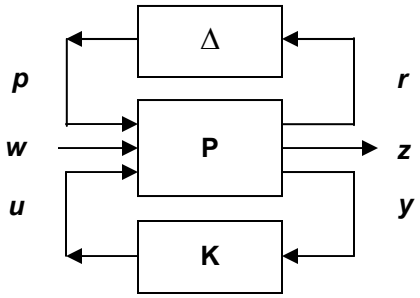

Figure 1. Standard form for robust design.

Mathematically, the general model is given by:

$$\begin{Bmatrix} \boldsymbol{r} \\ \boldsymbol{z} \\ \boldsymbol{y} \end{Bmatrix} = \begin{bmatrix} \mathbf{P}_{rp} & \mathbf{P}_{rw} & \mathbf{P}_{ru} \\ \mathbf{P}_{zp} & \mathbf{P}_{zw} & \mathbf{P}_{zu} \\ \mathbf{P}_{yp} & \mathbf{P}_{yw} & \mathbf{P}_{yu} \end{bmatrix} \begin{Bmatrix} \boldsymbol{p} \\ \boldsymbol{w} \\ \boldsymbol{u} \end{Bmatrix} = \mathbf{P} \begin{Bmatrix} \boldsymbol{p} \\ \boldsymbol{w} \\ \boldsymbol{u} \end{Bmatrix} \tag{11}$$

The main goal is remain the vector **z** small face to disturbances ***w*** and assure robustness. The classical H_∞ theory can be used to solve this problem, [4] or [8].

Problem: Find an output controller **K** such that:

$$\left\|\mathbf{H}_{zw}\right\|_\infty < \lambda \tag{12}$$

$$\left\|\mathbf{H}_{rp}\right\|_\infty \leq 1 \tag{13}$$

where λ is the cost of the design. The infinity norms above are related with the maximum gain for any transfer function, [4]. An additive uncertainty structure has been used in order to represent the unmodelled dynamic, Fig. 2. Mathematically, it can be written by:

$$\mathbf{G} = \mathbf{G}_c + \mathbf{G}_r \tag{14}$$

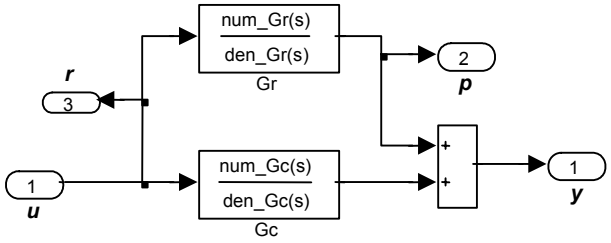

Figure 2. Additive uncertainty structure.

The transfer function $\mathbf{G_r}$ is relative to residual modes. In the present example this dynamic is known, but it is very complex to use in a controller design. So, a good way to overcome this difficulty it to replace it by a function with low order $\mathbf{G_p}$. It is possible due to small gain theorem, [4]. Thus:

$$\left\|\mathbf{G}_r\right\|_\infty \le \left\|\Delta\mathbf{G}_p\right\|_\infty, \quad \text{where } \left\|\Delta\right\|_\infty \le 1 \tag{15}$$

Once used a transfer function $\mathbf{G_p}$ as the uncertainty model, which satisfies the inequality (15), the order of controller would be lower. One disadvantage of this approach is relative to a very conservative procedure, but the time of design is reduced, [8].

The problem given by equations (12) and (13) can be solved by many different ways. One of them is by using the structured singular value theory (μ-synthesis). It consists in to change the standard form from robust and performance problem to a robust stability problem. However, in this procedure, the controller has high order and it can be difficult for practical implementation. There are some model reduction order techniques that can be used to overcome it, as for instance the Moore method. Unfortunately, these concepts are not well defined in literature for problems that involve uncertainties. Some authors use classical reductions to get low order controller designed by μ-synthesis procedure, as for example in [9].

An alternative way was proposed in [8] and [10], and it was adopted in the present paper. This approach is obtained by opening the feedback uncertainty block Δ loop and by adding the input and output related with an exogenous input and regulated output, respectively $\boldsymbol{w}'=[\boldsymbol{p}\ \boldsymbol{w}]^T$ and $\mathbf{z}'=[\boldsymbol{r}\ \boldsymbol{z}]^T$, where $\boldsymbol{z}=[\boldsymbol{u}'\ \boldsymbol{y}']^T$. To reduce the effect of the input $\boldsymbol{p}$ in the new regulated output an attenuation constant $\boldsymbol{K_d}$ is added to the input $\boldsymbol{p}$. In order to cancel this gain, it must be added an inverse gain in the output $\boldsymbol{r}$. Figure 3 shows the final generalized plant with the transfer function and respective input and outputs signal.

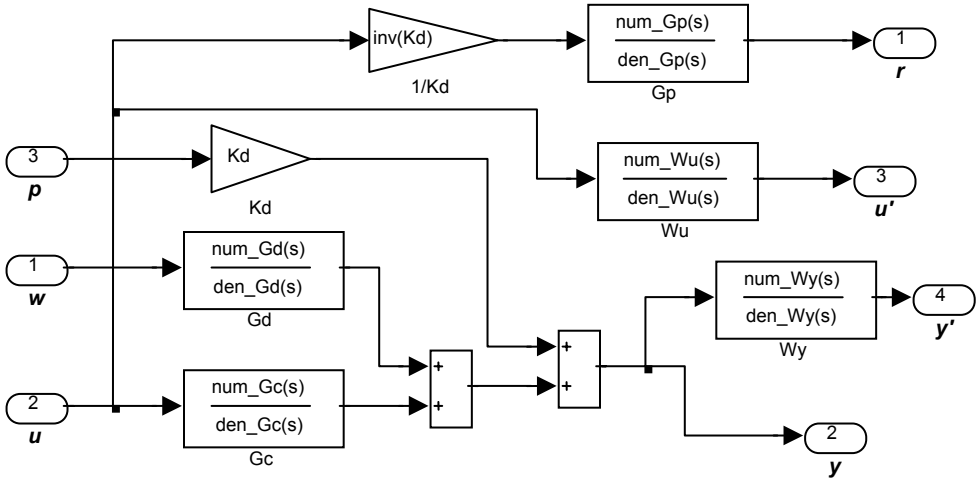

Figure 3. Generalized plant for robust problem used to design the controller.

The generalized plant has the following transfer functions matrix, [10]:

$$\mathbf{P}_{z'w'} = \begin{bmatrix} \mathbf{W}_y\mathbf{G}_d & \mathbf{W}_y\mathbf{K}_d \\ 0 & 0 \\ 0 & 0 \end{bmatrix}, \quad \mathbf{P}_{z'u} = \begin{bmatrix} \mathbf{W}_y\mathbf{G}_c \\ \mathbf{W}_u \\ \mathbf{G}_p\mathbf{G}_c\mathbf{K}_d^{-1} \end{bmatrix}$$
$$\mathbf{P}_{yw'} = \begin{bmatrix} \mathbf{G}_p & \mathbf{K}_d \end{bmatrix}, \qquad \mathbf{P}_{yu} = \mathbf{G}_c \tag{16}$$

where $\mathbf{G_d}$ is relative to disturbance input. The filters $\mathbf{W_y}$ and $\mathbf{W_u}$ are used to shape the regulated output. The filter $\mathbf{W}_y$ is often a low pass function in frequency domain and its objective is to increase the damping in the controlled

modes. The weighting function $\mathbf{W}_u$ is chosen in order to constrain the input control signal into the interested bandwidth. Substituting eq. (16) into eq. (11), replaced ***z*** by ***z***' and ***w*** by ***w***', it can be obtained, after some mathematical manipulation, the following equation in closed-loop:

$$\mathbf{H}_{z'w'} = \begin{bmatrix} \mathbf{W}_y & \mathbf{0} & \mathbf{0} \\ \mathbf{0} & \mathbf{W}_u & \mathbf{0} \\ \mathbf{0} & \mathbf{0} & \mathbf{G}_p\mathbf{K}_d^{-1} \end{bmatrix} \begin{bmatrix} \mathbf{S} & \mathbf{S} \\ \mathbf{U} & \mathbf{U} \\ \mathbf{U} & \mathbf{U} \end{bmatrix} \begin{bmatrix} \mathbf{G}_d & \mathbf{0} \\ \mathbf{0} & \mathbf{K}_d \end{bmatrix} \tag{17}$$

where **S** and **U** are the sensitivity and energy restriction functions, respectively. These functions are well known from classical control:

$$\mathbf{S} = \left(\mathbf{I} - \mathbf{G}_c\mathbf{K}\right)^{-1} \tag{18}$$

$$\mathbf{U} = \mathbf{K}\mathbf{S} \tag{19}$$

$\mathbf{W}_u$ and $\mathbf{G}_p$ are related with **U**, so, both functions can be used to restrict the input control signal. It occurres due the kind of unstructured uncertainty used (additive). Case one had been used, as for instance, multiplicative uncertainty the results would not be equals. Another important point is to observe that $\mathbf{W}_u$ is more related with uncertainties in high frequencies, due, mainly, to noise measurements. Usually, the dynamic uncertainty is well known (in our example $\mathbf{G}_r$ is known). So, the function $\mathbf{W}_u$ can be omitted in the design. The new configuration of the system is given by Fig. 4. In some cases it is needed to insert the attenuation gain $\mathbf{K}_w$ in the disturbance input to decrease the level of the exogenous signal that contribute to the response of the system, [10].

This augmented plant was done using toolbox LMI from Matlab with aid from *sconnect* command, [11]. The H_∞ problem, eq. (12) and (13), was solved using the command *hinflmi*, which applies convex optimization technique, [11] and [12].

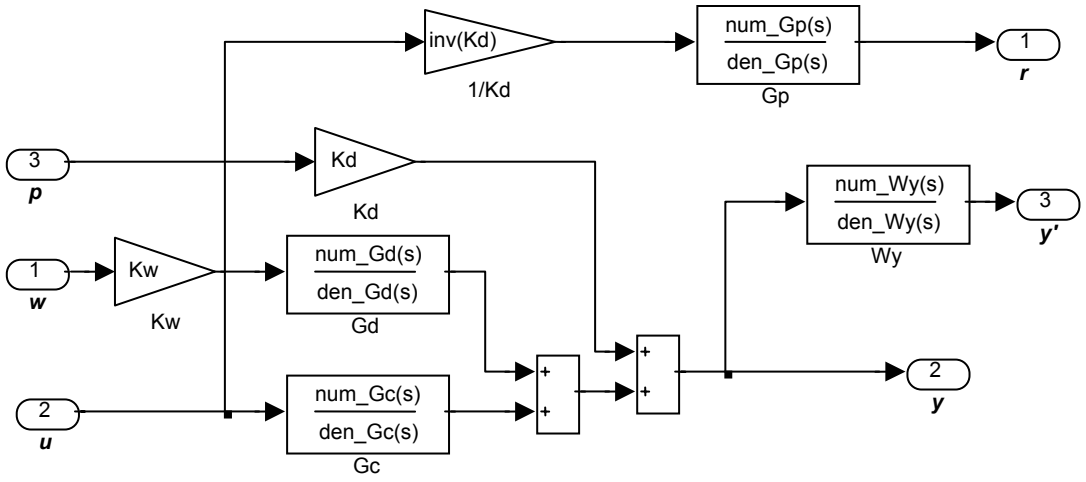

Figure 4. Augmented plant for robust problem used to design the controller.

NUMERICAL APPLICATTION

Flexible Truss Structure

In the numerical application is proposed the control design of a 2-bay truss structure with 31 bars, Fig. 5. At the principle, each truss member can be replaced by an active member. The nodes 1 to 4 are clamped. The materials properties and dimensions are given in Table 1. The tubes are made of steel with diameter of 6 mm and for each node there is a centralized mass block of 0.3 kg. It is considered that the damping is proportional to the stiffness and mass matrices ($\mathbf{D}=5.10^{-7}.\mathbf{K}+2.10^{-4}.\mathbf{M}$). The aim of these numerical investigations is to demonstrate the

applicability and efficiency of the theory shown in the previous sections. The state-space structural model is obtained through a program developed in Matlab® using finite element method (FEM).

Table 1. Material properties and dimensions of the smart truss structure

	Structure	Active Member
Elastic modulus (N/m^2)	2.1×10^{11}	5.26×10^{10}
Mass density (kg/m^3)	7800	7800
Cross-section area (m^2)	2.83×10^{-5}	3.85×10^{-5}
L (m)	0.25	0.15
Piezoelectric coefficient (N/V.m)	---	43.85
Dielectric coefficient (F/m)	---	2.124×10^{-8}

Each node has three degrees of freedom, translation in x, y and z direction, so, the truss structure has 24 active dofs, and the model in the form of states space results in order of 48. The control design to attenuate the vibration considers only the first two modes (4 states) of the structure, and the twenty-two remaining modes (44 states) are considered as residual modes in the model. In this application was considered the use of one “PZT wafer stack” and two sensors. The optimal placement of actuator and sensors are shown in Fig. 5.

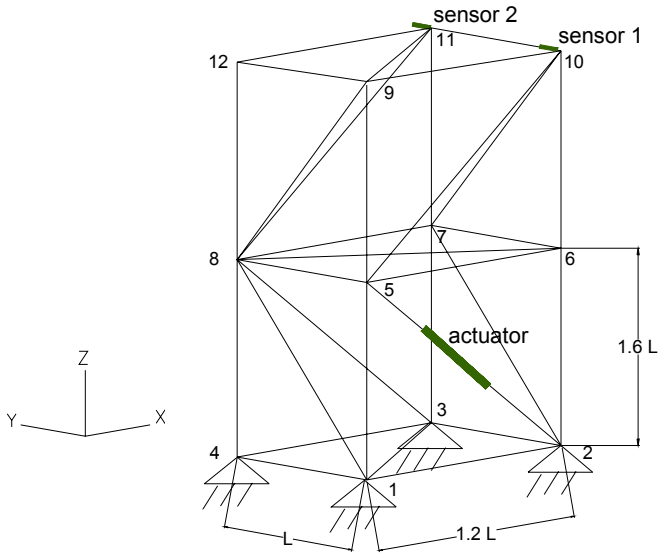

Figure 5. Truss structure showing the actuator and sensor location.

In this example, it is assumed that the piezoelectric actuator effect is not negligible, so, the dynamic properties of the truss structure change. As can be seen in the variation of the natural frequencies shown in the Table 2.

Table 2. Variation of the natural frequencies

	1°	2°	3°	4°	5°	6°
Truss	138.4	146.4	215.2	382.2	462.1	555.2
Smart Truss	138.9	155.5	217.0	382.8	468.3	570.2
Difference (%)	0.3	5.8	0.9	0.2	1.3	2.6

Placement of active members

The placement index of each candidate configuration with the objective to control the first two modes is shown in Fig. 6. The results are normalized with the maximum value set to unity. The largest value index for the placement index correspond to positions where the actuators and sensors are more effective.

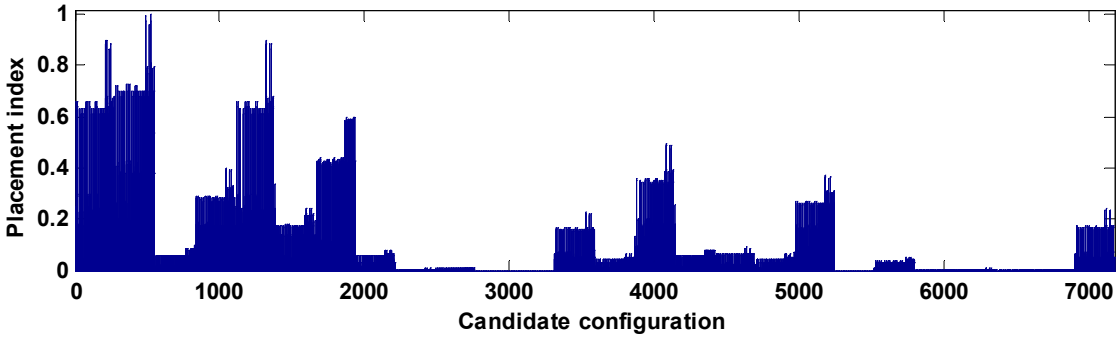

Figure 6. Placement index versus candidate configuration.

From Fig. 6 is possible to define the configuration where the system achieves the better performance. Table 3 shows the five better configurations of the sensors and actuators; the total numbers of possible configuration is 7176. The sensors are supposed to be positioned in the dofs of the nodes and the actuator between two nodes.

Table 3. Better configurations for sensors and actuator positions

Configuration candidate nº	Position of Sensor 1	Position of Sensor 2	Position of the Actuator	H_2 norm
527	node 10 y	node 11 y	nodes 2-5	4.888
493	node 9 x	node 11 y	nodes 2-5	4.825
489	node 9 x	node 10 x	nodes 2-5	4.746
490	node 9 x	node 10 y	nodes 2-5	4.745
520	node 10 x	node 11 y	nodes 2-5	4.745

Closed-loop Control

In this section, it was used the following configurations to verify the proposed methodology. The transfer function G_1, which is calculated by using an input at node 9 in y direction and measuring the response by a sensor at node 10 in y direction (sensor 1). The transfer function G_2 is calculated by using the actuator and sensor in the same position. Figure 7 shows the transfer function G_1 and G_2 for the nominal system, the reduced model, and residual model.

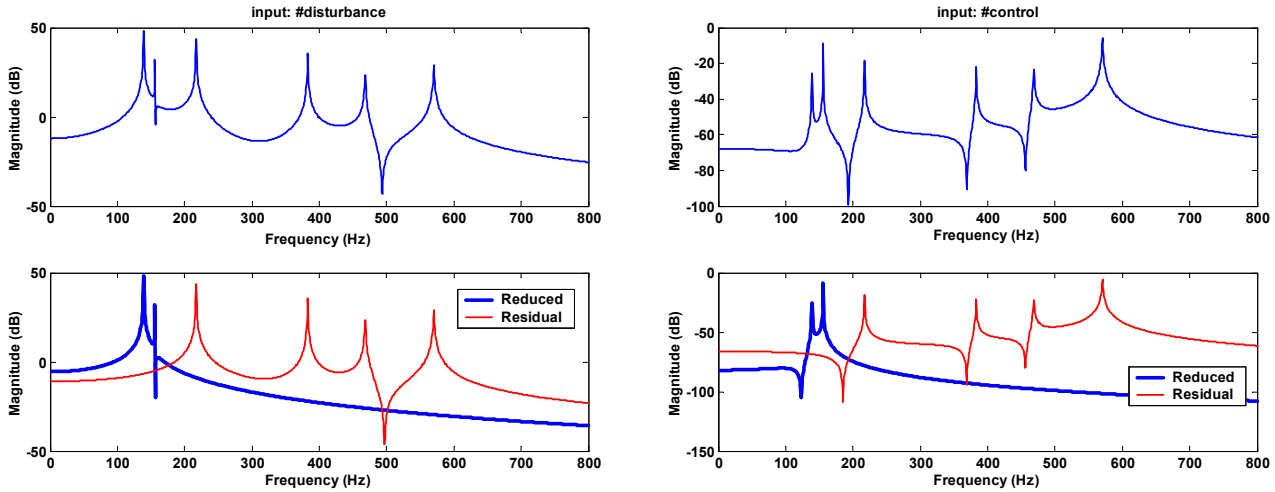

(a) Transfer function $\mathbf{G}_1$ for reduced and residual model.

(b) Transfer function $\mathbf{G}_2$ for reduced and residual model.

Figure 7. Magnitude plots of the FRF for G_1 and G_2.

In this methodology, the first step is to choose the $\mathbf{W}_y$ filter as a second order function with cut-off frequency between the first and the second natural modes. The unmodelled model is chosen by a low order model given by $\mathbf{G}_p$. The values of the gains used are $\boldsymbol{K_d}$= 0.02 and $\boldsymbol{K_w}$= 0.001. The transfer functions are given by:

$$\mathbf{W_y} = \frac{88.3}{s^2 + 188.5\,s + 8.9.10^5}, \qquad \mathbf{G_p} = 0.04\,\frac{\left(\omega_1^2 s^2 + \frac{2\zeta_1}{\omega_1}s + 1\right)^2}{\left(\omega_2^2 s^2 + \frac{2\zeta_1}{\omega_2}s + 1\right)^2} \tag{20}$$

where ω_1=754 rad/s, ω_2=2000 rad/s, ζ_1=0.1 and ζ_2=0.1. Figure 8 shows the singular value plot of these functions.

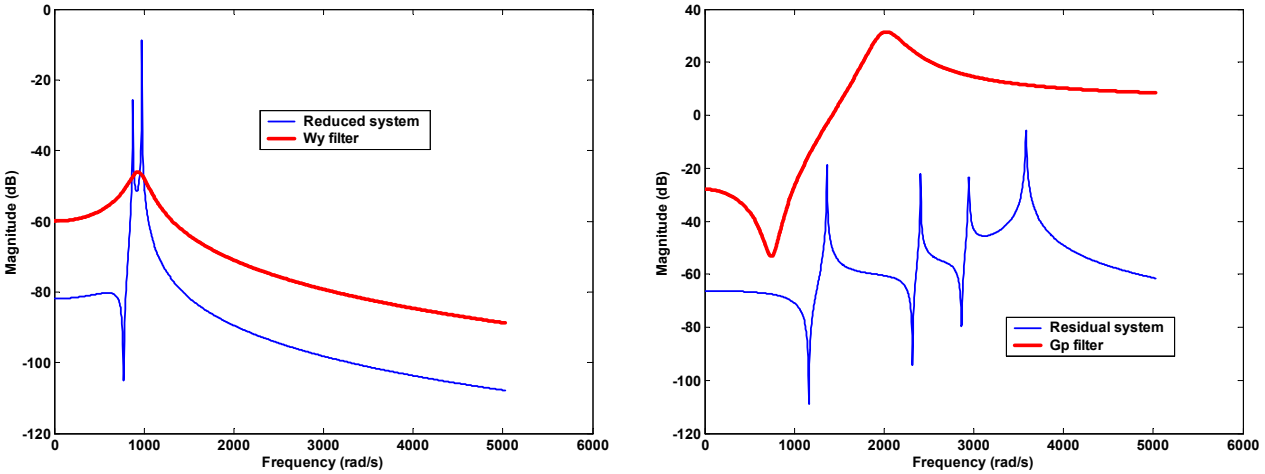

(a) Weighting function for the sensibility function. (b) Weighting function for the residual modes.

Figure 8. Singular value plots for weighting functions.

The closed-loop response (FRF between disturbance input ***w*** and output signal ***y***) of this system in frequency domain is shown in Fig. 9. There are a suitable amplitude attenuation in the two firsts modes and the other modes remain unaffected. The performance and robustness characteristics of the resulting controller are shown in Fig. 10. The specifications given by eq. (12) and (13) are reached, because the sensitivity function is limited by the inverse of filter $\mathbf{W}_y$ and the energy restriction function is limited by the inverse of $\mathbf{G}_p$, as shown in Fig. 10. Thus, despite of perturbations that may occurs due to residual modes, the system remains in acceptable levels in the resonance peaks.

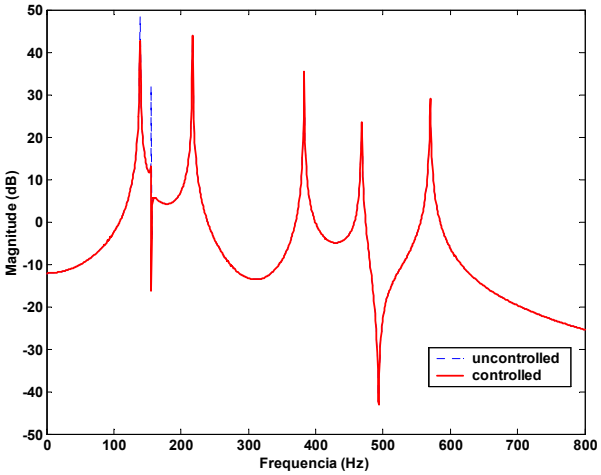

Figure 9. FRFs of the controlled and uncontrolled response.

When the system is controlled, the open loop value of the first mode attenuation reaches 6 dB. While the second mode an attenuation of 19 dB is achieved.

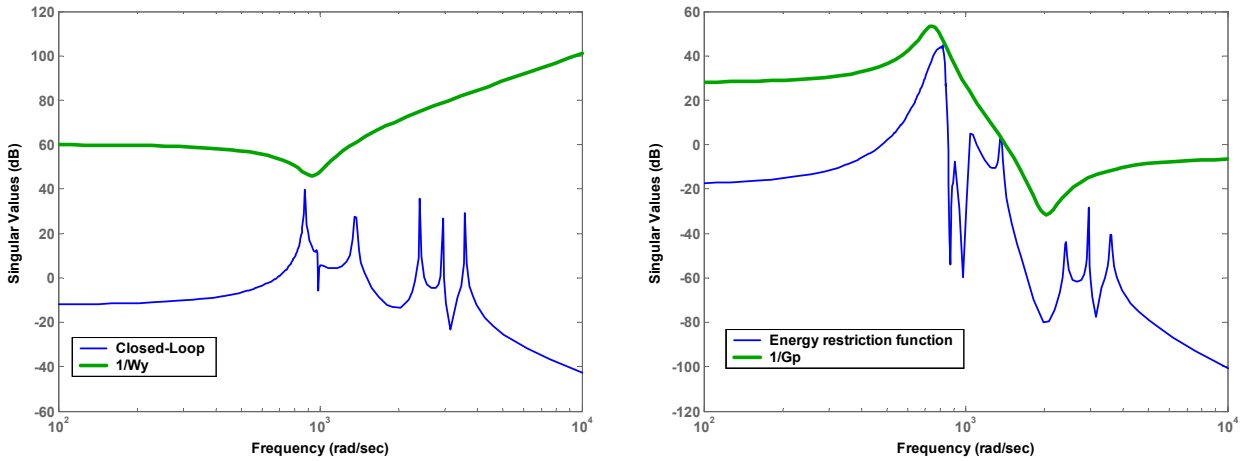

(a) **S** Sensitivity function (b) **U** Energy restriction function

Figure 10. Design performance and robustness.

Another important point can be understood by Fig. 10b; the large peaks correspond to low frequency modes, it means that input control signal can not be excited by the residual modes. The function **U** shows adequate robustness requirements.

CONCLUSION

When designing adaptive structures, the location of actuators must be chosen properly, because they can affect the efficiency of the control forces and the stability of the whole system. The applicability of the optimal placement theory, using the H_2 norm technique, considering the two first modes of the structure, was shown through an example in a truss structure with 7176 candidate configurations for two sensors and one actuator.

An H_∞ output feedback control strategy was used actively to control the first two modes of a spatial truss structure with 31 bars. The spillover problem due to unmodelled modes was suppressed. The first two modes were controlled in a satisfactory way, and the other ones are nearly the same as those when the control system is open loop.

ACKNOWLEDGEMENT

The authors would like to acknowledge the financial support from Research Foundation of the State of São Paulo (FAPESP-Brazil)

REFERENCES

[1] Ruggiero, E. J., *Active Dynamic Analysis and Vibration Control of Gossamer Structures Using Smart Materials*. MS thesis, Virginia Polytechnic Institute and State University, Blacksburg/VA, 2002.

[2] Yan., Y. J. and Yam, L. H., *A Synthetic Analysis on Design of Optimum Control for an Optimized Intelligent Structure*, Journal of Sound and Vibration, Vol. 249, No 4, pp. 775-784, 2002.

[3] Sadri, A. M., Wrigth, J. R., and Wynne, R. J., Modelling and optimal placement of piezoelectric actuator in isotropic plates using genetic algorithms. *Smart materials and structures*, vol.8, pp. 490-498, 1999.

[4] Burl, J. B., *Linear Optimal Control: H_2 and H_∞ Methods*, Addison-Wesley, 1999.

[5] Lammering., R., Jia, J. and Rogers, C. A., “Optimal Placement of Piezoelectric Actuators in Adaptative Truss Structures”, Journal of Sound and Vibration,vol.171, n. 1, pp. 67-85, 1994.

[6] Gawronski, W., Dynamics and Control of Structures: A Modal Approach, 1.ed. New York: Springer Verlag, 231p, 1998.

[7] Assunção, E., Marchesi, H. F.,Teixeira, M. C. M. and Peres, P. L. D., Otimização global rápida para o problema de redução H_∞ de modelos. *XIV Congresso Brasileiro de Automática*, Natal - RN, in CD-Room, 2002.

[8] Moreira, F. J. O., Arruda, J. R. F. and Inman, D. J., Design of Reduced Order H_∞ Controller for Smart Structures, *17th Biennial Conference on Mechanical Vibration and Noise*, pp. 1-9*,* 1999.

[9] Abreu, G. L. C. M, *Projeto Robusto H_∞ Aplicado no Controle de Vibrações em Estruturas Flexíveis Com Materiais Piezelétricos Incorporados*, Ph.D. Dissertation, Universidade Federal de Uberlândia, Brazil, 2003.

[10] Moreira, F. J. O., Arruda, J. R. F. and Inman, D. J., *Design of a Reduced Order H infinity Controller for Smart Structure Satellite Applications*, Philosophical Transaction of the Royal Society, V.359, No.1788, pp. 2251-2270, 2001.

[11] Gahinet., P., Nemirovski, A., Laub, A. J. and Chiliali, M., *LMI Control Toolbox User’s Guide*. The Mathworks Inc., Natick, MA, USA, 1995.

[12] Gahinet, P. and Apkarian, P., *A Linear Matrix Inequality Approach to H_∞ Control,* International Journal Robust and Nonlinear Control, vol.4, pp. 421-448, 1994.